JOURNAL OF APPLIED ELECTROCHEMISTRY **28** (1998) 423–431

Electrochemical membranes: transport limitations for absorbed gases

L. J. FORNEY, C. L. HENDERSON

School of Chemical Engineering, Georgia Institute of Technology, Atlanta, GA 30332, USA

Received 8 November 1996; revised 28 May 1997

The physics of a gas diffusion electrode–membrane cell is discussed and comparisons are made with experimental data. In particular, a second order expansion has been used to correlate the maximum current density data, valid for both small to large overpotentials and electrode specific surface areas. It is also demonstrated that the limiting or maximum current density for the diffusion limit can be predicted by assuming simple molecular diffusion across the membrane and the ion reference (open circuit) concentration in the cathode. An expression is also developed to account for differences in reactant gas concentrations and flowrates between reference and normal operating conditions. Comparisons are made between the theory and maximum current data for the absorption of H_2S, CO_2 and SO_2. These comparisons suggest that the current density limitations of the cell are affected by electrochemical reaction rates on the cathode surface. Other possible limitations for electrochemical cell performance are discussed.

Keywords: *membrane*, *electrochemical*, *molten salt*, *separation and gas diffusion electrode*

List of symbols

A_c	cross-sectional area of cathode (cm^2)
a_c	specific surface area of the cathode ($cm^2\ cm^{-3}$)
c_i	concentration of species i ($mol\ cm^{-3}$)
c_0	inlet reactant gas phase concentration (ppm)
c_0^*	reference inlet gas phase concentration (ppm)
c_f	outlet reactant gas phase concentration (ppm)
c_f^*	outlet reactant gas phase concentration (ppm)
c_{sr}	reference concentration of the dissolved reactant ($mol\ cm^{-3}$)
c_s	concentration of dissolved gas phase reactant ($mol\ cm^{-3}$)
$\bar{c}_s$	average concentration of dissolved reactant ($mol\ cm^{-3}$)
$\bar{c}_{sr}$	average reference concentration of dissolved reactant ($mol\ cm^{-3}$)
c_{lr}	reference concentration of the current-carrying ion ($mol\ cm^{-3}$)
c_{10}	concentration of the current-carrying ion at $x = 0$
c_{3L}	concentration of the positive supporting ion at $x = L$ ($mol\ cm^{-3}$)
D_i	diffusion coefficient of species i ($cm^2\ s^{-1}$)
F	Faraday's constant ($9.648 \times 10^4\ C\ mol^{-1}$)
h_c	thickness of the cathode (cm)
h_s	thickness of the membrane (cm)
i	current density ($mA\ cm^{-2}$)
i_m	maximum current density ($mA\ cm^{-2}$)
i_r	exchange current density ($mA\ cm^{-2}$)
I	normalized current density
I_m	maximum value of I
K_a	normalized cathode specific surface area
K_c	normalized reference concentration c_{1r} of current carrying ion
K_h	the ratio membrane thickness : cathode thickness
L	thickness of the cathode and membrane ($h_c + h_s$) (cm)
M	molarity ($mol\ L^{-1}$)
M_w	molecular weight ($g\ mol^{-1}$)
P	total pressure (atm)
R	universal gas constant
T	absolute temperature (K)
V	volume flowrate of gas ($cm^3\ min^{-1}$)
V^*	reference volume flowrate of gas ($cm^3\ min^{-1}$)
x	normalized spacial coordinate ($= x_0/h_c$)
x_0	spacial coordinate (cm)
x_{max}	molar fraction of gas phase reactant removed by current
y	potential function
y_c	potential function at the cathode–membrane interface
y_0	potential function at $x = 0$
z_i	absolute value for the charge number of species i

Greek symbols

ε	porosity of the electrolyte
Ψ	normalized solution potential
φ	solution potential (V)
τ	tortuosity of electrolyte
ρ	density ($g\ cm^{-3}$)

Superscripts and subscripts

c	cathodic region
L	position $x = L/h_c$
m	maximum or limiting current
0	position $x = 0$
r	reference value
s	membrane region
1	current-carrying ion
2	negative component of supporting electrolyte
3	positive component of supporting electrolyte

1. Introduction

In a gas diffusion electrode the electrolytic solution partially penetrates the void spaces of a porous matrix. This provides a mechanism for the mass transport of gaseous reactants through gas-filled pores by diffusion to the electrolyte film where the reactant gas is absorbed. Relative to solid electrodes, the porous electrodes provide much larger contact areas per unit volume between the electrolyte, absorbed gas and solid electronic conductor. Ions in the electrolyte must also diffuse through the liquid solution in both electrode and an attached porous flooded membrane or separator. The matrix separator or membrane is designed to retain the electrolyte and prevent electrolyte pore flooding by capillary action into the cathode. It is the relative rates of the gas and ion diffusion compared to the electrochemical reactions in such a cell that determine the potential–current characteristics and ultimately the limiting current.

A large class of industrially important electrochemical reactions involve the use of gas diffusion electrodes. For example, certain fuel cells use gas-fed porous electrodes attached to an ion exchange membrane. Recent numerical works describing the operating characteristics of ion exchange membrane fuel cells are those of Bernardi and Verbrugge [1] and Ridge *et al.* [2] where the former included the effects of electroosmotic convection. Another class of fuel cells that use molten salt in place of an aqueous electrolyte has also been analysed [3].

Other potential applications for gas diffusion electrode–membrane cells are in gas purification and separation processes. These electrochemical cells may be advantageous, providing high selectivity at low cost for either the removal of oxygen or carbon dioxide from air or the separation of hydrogen sulfide or sulfur dioxide [4–7].

A numerical simulation of the transport rate of ions through a gas diffusion cathode–membrane cell was conducted by Mao *et al.* [8]. In this study the time-dependent parabolic partial differential equations representing the conservation of gas and ion component including reversible Butler–Volmer kinetics in an immobile supporting electrolyte were solved. Analytical expressions were developed recently by Forney [9] to predict ion current limitations for a gas diffusion electrode attached to a flooded membrane. Conservation expressions were solved for reversible electrochemical reactions (oxidation–reduction) in the presence of a stationary supporting electrolyte. Assuming that the gaseous reactant and product diffusion times are much smaller than the ion transfer step, maximum current densities were presented corresponding to either a reaction or larger ion diffusion limit where the latter case provides current reversal in the cathode. It was demonstrated that the distinction between both cases disappears if the ratio of the membrane thickness to the reaction penetration depth based on the exchange current is larger (large cathode specific surface area). An asymptotic formula for the maximum current, valid for both low and high overpotentials, was derived that depends on a normalized reactant concentration (overpotential), membrane-to-cathode thickness and the ratio of ion diffusion-to-reaction time.

In the present study the formula for maximum current, valid for both large and small cathode specific surface areas, has been compared with experimental data. The data consist of maximum current densities formed by the absorption of either carbon dioxide, hydrogen sulfide or sulfur dioxide in alkali metal salt electrolytes at low to moderate overpotentials [6, 7, 10]. Moreover, a Taylor series expansion for the maximum current density has been derived that is valid for low overpotentials and a simple interpretation of the physics is discussed. The series expansion provides a useful estimate of the maximum current density under optimum conditions and problems associated with achieving these limits are discussed.

2. Theory

In the discussion that follows, it is assumed that the reactant gas diffuses into the pores of the cathode and dissolves in the electrolytic liquid phase that forms a thin film on the solid surface of the porous cathode as indicated in Fig. 1. The electrochemical reaction (reduction) of the dissolved reactant gas at the cathode surface produces the negative-current carrying ion that is transported largely by diffusion to the anode in a supporting stationary electrolyte. It is also assumed that electroosmotic convection of the electrode can be neglected.

2.1. *Maximum current*

We now assume that the net formation of the current density per unit length in the cathode is the result of the reduction of the absorbed gas in solution. Writing the product of the Butler–Volmer equation and specific surface area of the cathode a_c, one obtains

$$\frac{dI}{dx} = \frac{a_c i_r h_c^2}{3FD_1^e c_{3L}} \left(\frac{c_s}{c_{sr}} e^{\Psi} - \frac{c_1}{c_{1r}} e^{-\Psi} \right) \qquad (1)$$

where i_r is the exchange current density at the reference concentrations of both the absorbed gas c_{sr} and

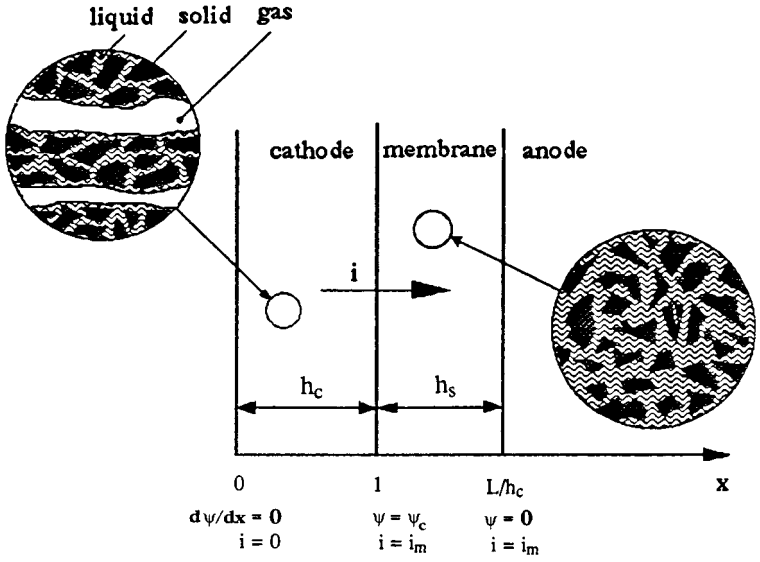

Fig. 1. Schematic of gas diffusion electrode–membrane cell.

current-carrying ion c_{1r} and c_s is the concentration of the dissolved reactant in equilibrium with the pore gas phase. The normalized solution potential (overpotential) is written in the form

$$\Psi = \left(\frac{F}{RT}\right)(\varphi - \varphi_c + \varphi_e) \tag{2}$$

where the solution potential φ has been referenced with the cathode solid matrix potential φ_c and an equilibrium potential φ_e evaluated at reference electrolyte concentrations. The variable c_1 is the concentration of the current carrying ion at limiting conditions (maximum current) when $\Psi = c_1 = 0$ at the anode [11, 12]. In this case,

$$\frac{c_1}{c_{3L}} = \left(\frac{Z_3}{Z_1}\right)\left(e^{-z_3\Psi} - e^{z_2\Psi}\right) \tag{3}$$

The remaining variable is the normalized current density

$$I = \frac{ih_c}{3FD_1^c c_{3L}} \tag{4}$$

where c_{3L} is the reference concentration of the positive supporting electrolyte in the anode at $x = L/h_c$.

In the following discussion, we consider a negative current carrying ion of concentration c_1 with a valence of -2 or $Z_1 = 2$ where Z_i is the absolute value of the charge number for species i. Moreover, the current carrying ion is suspended in a supporting alkali metal salt consisting of species $M^{2-}(Z_2 = 2)$ and $M^{+}(Z_3 = 1)$ of concentration c_2 and c_3, respectively. It is also useful to define a dependent variable in Equations 1 and 3:

$$y = e^{-\Psi} \tag{5}$$

Substituting $Z_3 = 1$ and $Z_1 = Z_2 = 2$ in the Butler–Volmer equation (1) and noting that $dy/dx = -I$ and $dI/dx = (dI/dy)(dy/dx)$ across the cathode, the conservation of current becomes [9]

$$I\frac{dI}{dy} = K_a\left[y^2 - (1 + K_c)y^{-1}\right] \tag{6}$$

subject to the boundary conditions

$$y = y_0, \quad I = 0 \tag{7a}$$

$$y = y_c, \quad I = I_m \tag{7b}$$

Here, y_0 is the overpotential necessary to maintain zero current ($I = 0$) on the gas side of the cathode at $x = 0$ or from Equation 6

$$y_0 = (K_c + 1)^{1/3} \tag{8}$$

The remaining boundary condition, y_c, is the overpotential for maximum current at the cathode membrane interface at $x = 1$ defined as

$$y_c = I_m K_h + 1 \tag{9}$$

Other dimensionless groups are the ratio of cathode thickness, h_c, to the reaction penetration depth (based on the exchange current)

$$K_a = \frac{a_c i_r h_c^2}{6FD_1^c c_{1r}} \tag{10}$$

the normalized reactant concentration

$$K_c = 2\left(\frac{c_{1r}}{c_{3L}}\right)\left(\frac{c_s}{c_{sr}}\right) \tag{11}$$

and the dimensionless ratio of membrane to cathode thickness

$$K_h = \left(\frac{h_s}{h_c}\right)\left(\frac{D_1^c}{D_1^s}\right) \tag{12}$$

Here, D_1^s is the effective diffusivity of the current carrying ion in the membrane where $D_1^s = D_1^0(\varepsilon/\tau)$.

Integrating Equation 6, a closed-form analytical expression is obtained for the maximum current density in the cell:

$$\frac{I_m^2}{2} - K_a\left[\frac{1}{3}\left(y_c^3 - y_0^3\right) - (K_c + 1)\ln\left(\frac{y_c}{y_0}\right)\right] = 0 \tag{13}$$

In Equation 13, the maximum current density, I_m, must be determined by locating two real roots cor-

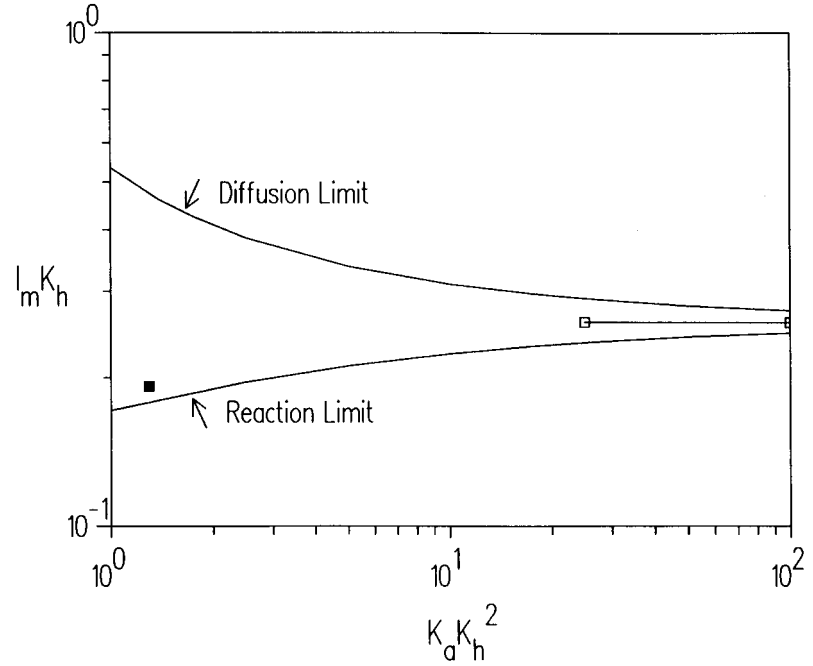

Fig. 2. Normalized current limit against the ratio ion diffusion: reaction time. $K_c = 1.0$. Key: (—) theory; (□) $(K_c + 1)^{1/3} - 1$; (■) Mao, Adanuvor and White (1990).

responding to either the reaction and diffusion limits Forney [9]. Further analysis of Equation 13 illustrates that the two roots for the maximum current converge with increasing cathode specific surface areas. These features are illustrated in Fig. 2. In this case the electrolytic reaction occurs uniformly across the cathode and $y_0 \simeq y_c$.

2.2. *Dissolved reactant concentration*

The analysis in Section 2.1 assumed that the gas phase reactant concentration was uniform across the face of the cathode. All gradients in concentration were therefore in the direction of the current. In practice, the reactant gas flows into the cell at the inlet and passes across the cathode face to the outlet resulting in a decrease in the gas concentration. Since the dissolved reactant concentration, c_s, is assumed to be in equilibrium with the gas phase, there may be variations in c_s along the cathode face. Therefore, the ratio c_s/c_{sr} that appears in the normalized reactant concentration K_c, defined by Equation 11, must be interpreted as the ratio of average values. The dissolved concentration ratio c_s/c_{sr}, is also strongly influenced by the initial gas phase concentrations during operation of the cell at both maximum and open circuit or reference conditions and also by the relative magnitudes of both the maximum and reference current densities.

The average reactant gas phase concentration are defined as

$$\bar{c} = \frac{c_0 + c_f}{2}, \quad \bar{c}^* = \frac{c_0^* + c_f^*}{2} \tag{14}$$

where c_0, c_f are the inlet and outlet reactant gas phase concentration and c_0^* represents reference conditions. Since $\bar{c}/\bar{c}^* = \bar{c}_s/\bar{c}_{sr}$ at equilibrium, Equation 14 gives the dissolved concentration ratio

$$\frac{\bar{c}_s}{\bar{c}_{sr}} = \frac{c_0}{c_0^*}\left(\frac{1 + c_f/c_0}{1 + c_f^*/c_0^*}\right) \tag{15}$$

A molar balance can also be related to the current densities in the form

$$\frac{i_m}{i_r} = \frac{c_0 V(1 - c_f/c_0)}{c_0^* V^*(1 - c_f^*/c_0^*)} \tag{16}$$

where V is the volume flow rate of gas through the cell. Substituting for c_f^*/c_0^* from Equation 16 into Equation 15, gives

$$\frac{\bar{c}_s}{\bar{c}_{sr}} = \frac{c_0}{c_0^*}\left(\frac{c_f/c_0 + 1}{2 + \left(\frac{i_r}{i_m}\right)\left(\frac{c_0 V}{c_0^* V^*}\right)(c_f/c_0 - 1)}\right) \tag{17}$$

The lower limit in Equation 17 occurs when $i_r/i_m \to 0$ and $c_f/c_0 \to 0$ or $\bar{c}_s/\bar{c}_{sr} > (1/2)(c_0/c_0^*)$. The upper limit occurs when the volume flowrate of gas at maximum current conditions is large or $c_0 V/c_0^* V^* \to \infty$. In the latter case, $c_f/c_0 \to 1$ and $i_r/i_m \to 0$ or $\bar{c}_s/\bar{c}_{sr} < c_0/c_0^*$. In summary, the ratio of dissolved reactant gas concentrations is bounded by the following:

$$\frac{1}{2}\frac{c_0}{c_0^*} < \frac{\bar{c}_s}{\bar{c}_{sr}} < \frac{c_0}{c_0^*} \tag{18}$$

subject to the solubility limits of the gas. In addition, Equation 17 provides a useful expression to evaluate experimental values of $\bar{c}_s/\bar{c}_{sr}$ in terms of current densities.

2.3. *Asymptotic formula*

It is useful to expand the maximum current density given by Equation 13 in a Taylor series about the

point $K_c = 0$ corresponding to zero overpotential at the cathode. In this limit both K_c and $I_m K_h \ll 1$ in Equations 8 and 9 lead to the approximation in Equation 13 for the term $\ln(y_c/y_0) \sim I_m K_h - K_c/3 + 0(K_c^2)$. Expansion of Equation 13 to second order accuracy in K_c yields the kinetic limit

$$\frac{I_m^2}{2} = K_a\left[-I_m K_h K_c + \frac{3}{2} I_m^2 K_h^2 + \frac{K_c^2}{6} + 0\left(K_c^3\right)\right]$$

Thus, the maximum kinetic limit is

$$I_m K_h = \frac{K_c}{3}\left[\frac{\left(3K_a K_h^2\right)^{1/2} - 3K_a K_h^2}{1 - 3K_a K_h^2}\right] \qquad (19)$$

for K_c, $K_a K_h^2 \ll 1$. In Equation 19, the normalized cathode specific surface area $K_a K_h^2$ can be described as either the ratio of membrane thickness h_s to the reaction penetration depth or, in simple terms, the ratio of diffusion time across the membrane to ion reaction time in the cathode. Therefore, if $K_a K_h^2 \gg 1$ the cell is diffusion limited while $K_a K_h^2 \ll 1$ corresponds to the reaction limited case.

Another useful limit of Equation 13 corresponds to large cathode specific surface area $K_a K_h^2 \gg 1$ or the diffusion limit as shown on the right of Fig. 2. In this case $y_0 \simeq y_c$ and an expression for the maximum current, valid for all K_c, in the form

$$I_m K_h = (K_c + 1)^{1/3} - 1 \quad \text{for } K_a K_h^2 \gg 1 \qquad (20)$$

is obtained. It is useful to note that Equation 20 reduces to

$$I_m K_h = \left[\frac{K_c}{3}\right] + 0\left(K_c^2\right) \quad \text{for } K_c \ll 1 \qquad (21)$$

and that $I_m K_h \to K_c/3$ for $K_a K_h^2 \gg 1$ in Equation 19.

These results and numerical root searching methods suggest that the expression below for the maximum current density is valid to within 10% for all values of both the overpotential K_c and $K_a K_h^2$ corresponding to the lower reaction limit in Fig. 2, or

$$I_m K_h = \left[(K_c + 1)^{1/3} - 1\right]\left[\frac{\left(3K_a K_h^2\right)^{1/2} - 3K_a K_h^2}{1 - 3K_a K_h^2}\right] \qquad (22)$$

Substituting for the dimensionless groups I_m, K_h and K_c in the first term of the series in Equation 21, gives an expression for the maximum current density

$$I_m = \frac{2c_{1r} F D_1^s}{h_s}\left(\frac{\bar{c}_s}{\bar{c}_{sr}}\right) \qquad (23)$$

This implies that the limiting mass transport of the current carrying ion (valence of -2 in this study) can be viewed as simple Fickian diffusion across the membrane bounded by the reference (open circuit) concentration of the current carrying ion in the cathode as shown in Fig. 3. The ratio $\bar{c}_s/\bar{c}_{sr}$ of the dissolved reactant gas is the exposure factor due to nonuniform gas properties (i.e., reactant gas phase concentrations, volume flow rates etc.) between the reference (open circuit) and actual test conditions as discussed in Section 2.2.

3. Experimental results

3.1. *Cathode reactions and surface area*

Electrochemical membranes have been tested recently for the selective removal of H_2S [6, 7, 10, 13–15]. Although there may be a number of possible reaction mechanisms occurring within the catholyte, the net cathode reactions are listed below that produce the indicated current carrying ion on the right. Also included in the list is the possible reduction of CO_2 and steam to carbonate [7].

For H_2S:

$$H_2S + 2e^- \longrightarrow H_2 + S^{2-} \qquad (24)$$

For CO_2:

$$CO_2 + H_2O + 2e^- \longrightarrow CO_3^{2-} + H_2 \qquad (25)$$

For SO_2:

$$SO_3 + \tfrac{1}{2}O_2 + 2e^- \longrightarrow SO_4^{2-} \qquad (26)$$

In the last reaction it is assumed that the SO_2 has been preoxidized to SO_3 before entering the cell.

The electrolyte used for Reactions 24 and 25 was an alkali metal eutectic composed of Li_2CO_3–K_2CO_3 with a cation molar ratio 62% Li^+/38% K^+. These reactions occurred at cell temperatures of 610–650 °C. Sulfur dioxide removal occurred with potassium pyrosulfate ($K_2S_2O_7$) with 5–10% V_2O_5 on a weight basis at cell temperatures of 400 °C.

The solid matrix used to immobilize the molten electrolyte must prevent flooding from the membranes into the cathode which would fill the gas pores and reduce the gas interfacial area. Moreover, the specific surface area of the cathode, a_c, should be large enough to insure that the electrochemical reaction times within the cathode do not limit the current production within the cell. The maximum specific surface area, a_c (area per unit volume), of the cathode was estimated to be about $10^3\,cm^2\,cm^{-3}$. In practice, because of partial pore flooding, the possible range of values of the specific surface area is estimated to be $10\,cm^2\,cm^{-3} < a_c < 10^3\,cm^2\,cm^{-3}$. In the present study, a constant value $a_c = 100\,cm^2\,cm^{-3}$ was assumed. Assuming an exchange current (reference) $i_r \sim 1\,mA\,cm^{-2}$, a cathode thickness, h_c, about 0.08 cm, a membrane thickness $h_s = 0.2$ cm, an ion diffusivity, D_1^c, about $10^{-5}\,cm^2\,s^{-1}$ and a reference concentration of the current carrying ion, c_{1r}, about 10 M (see Table 1) the dimensionless group $K_a K_h^2 \sim 0.1$ as defined by Equations 10 and 12. These results suggest that the current density limitations of the cell were affected by electrochemical reaction rates on the cathode surface.

3.2. *Ion diffusivity*

Limited information exists concerning values of the diffusivity of sulfide, sulfate or carbonate in molten alkali metal salts. In the present study the results

Table 1. Summary of experimental data

Author	*Run*	*Gas*	$10^5 D_l^s$ /cm^2 s^{-1}	c_{1r} /M cm^{-3}	c_{3L} /M cm^{-3}	c_0 /ppm	V /cm^3 min^{-1}	*% Gas* (i_r) *removal*	*% Gas* (i_m) *removal*	$\bar{c}/\bar{c}^*$	i_r/mA cm^{-2}
Alexander	1	H_2S	1.08	0.012	0.04	2000	109	50	80	0.80	1.81
Alexander	2	H_2S	1.08	0.012	0.04	2000	109	42	62	0.87	1.52
Alexander	13	H_2S	1.08	0.012	0.04	2000	105	33.8	88.5	0.67	1.18
Weaver	41	CO_3	0.85	0.016	0.04	350000	30	40.5	55	0.90	31.4
Weaver	43	CO_3	0.85	0.016	0.04	350000	45	28	65	0.78	32.6
Alexander	13	CO_3	0.85	0.016	0.04	10000	105	25	86	0.65	4.35
Alexander	13	H_2S	1.08	0.012	0.04	2000	105	33.8	88.5	0.67	1.18
Alexander	14	CO_3	0.85	0.016	0.04	1000	104	8	58.3	0.68	1.38
Alexander	14	H_2S	1.08	0.012	0.04	2000	104	62.5	89.7	0.80	2.15
Alexander	16	CO_3	0.85	0.016	0.04	13700	104	17	71	0.64	2.93
Alexander	16	H_2S	1.08	0.012	0.04	3000	109	48.6	79.3	0.79	1.75
Alexander	24	H_2S	1.08	0.012	0.04	3000	109	19	98	0.56	15
Alexander	1	SO_2	0.85	0.0014	0.019	3000	35.0	1	97	0.52	0.133
McHenry	2	SO_2	0.85	0.0014	0.019	3000	36.5	1	90	0.55	0.133

Author	*Run*	*Gas*	i_m/mA cm^{-2}	h_c/cm	h_s/cm	*Cathode diam.*/cm	$10^2 K_a^*$	K_c	K_h	I_m	I_m (*theory*)
Alexander	1	H_2S	2.89	0.08	0.2	3.18	0.015	0.480	2.5	0.0018	0.055
Alexander	2	H_2S	2.24	0.08	0.2	3.18	0.012	0.524	2.5	0.0042	0.060
Alexander	13	H_2S	3.08	0.08	0.2	3.18	0.0098	0.402	2.5	0.0058	0.047
Weaver	41	CO_3	42.6	0.08	0.2	4.76	0.196	0.727	2.5	0.0341	0.079
Weaver	43	CO_3	75.6	0.08	0.2	4.76	0.203	0.627	2.5	0.0606	0.070
Alexander	13	CO_3	14.9	0.08	0.2	3.18	0.027	0.521	2.5	0.0120	0.060
Alexander	13	H_2S	3.08	0.08	0.2	3.18	0.0098	0.402	2.5	0.0019	0.047
Alexander	14	CO_3	10.0	0.08	0.2	3.18	0.0086	0.545	2.5	0.0080	0.062
Alexander	14	H_2S	3.0	0.08	0.2	3.18	0.0178	0.481	2.5	0.0019	0.056
Alexander	16	CO_3	12.8	0.08	0.2	3.18	0.0173	0.516	2.5	0.0103	0.059
Alexander	16	H_2S	2.86	0.08	0.2	3.18	0.0145	0.478	2.5	0.0018	0.055
Alexander	24	H_2S	77.8	0.08	0.2	3.18	0.124	0.338	2.5	0.0491	0.040
Alexander	1	SO_2	12.5	0.08	0.2	3.18	0.0095	0.078	2.5	0.0175	0.025
McHenry	2	SO_2	11.6	0.08	0.2	3.18	0.0095	0.083	2.5	0.0162	0.025

*$a_c = 10^2$ cm^2 cm^{-3}

compiled by Janz and Bansal [16] were used for the diffusivity of carbonate in a Li_2CO_3–K_2CO_3 eutectic over a temperature range 850 to 980 K. For example, at 925 K D_l^0 for CO_3^{2-} is approximately 1.42×10^{-5} cm^2 s^{-1}. If the ratio of porosity to tortuosity, ε/τ, in the membrane is about 0.6, the value of $D_l^s(CO_3^{2-})$ is about 1.08×10^{-5} cm^2 s^{-1}, as shown in Table 1. Since no information exists for the diffusivity of sulfide, we assume the Wilke–Chang correlation $D \alpha 1/V_a^{0.6}$ where V_a is the solute molar volume [17]. The ratio carbonate : sulfide molar volumes provides an estimate of $D_l^s(S^{2-})$ of 1.08×10^{-5} cm^2 s^{-1}. These values were also used to estimate D_l^0 within the cathode.

3.3. *Data correlation*

The experiments described in Section 3.1 and summarized in Table 1 characterize the electrochemical cell performance. The percentage removal of the reactant gas was recorded with increasing applied current across the cell. An estimate was then made of the maximum removal rate of the reactant gas (e.g., H_2S) for the selected runs listed in Table 1. The reference or exchange current and maximum current density were computed from Equation 27 [6]

$$i_m = \frac{PVx_{max}2F}{A_c RT} \tag{27}$$

where F is Faraday's constant, x_{max} is the maximum molar fraction of species removed, $P = 1$ atm and A_c is the cross-sectional area of the cathode.

Knowledge of the flow rates, inlet and outlet gas compositions and the ratio reference: maximum current densities provide values of the ratio of average dissolved reactant concentrations $\bar{c}_s/\bar{c}_{sr}$ from Equation 17. For the experiments listed in Table 1, the inlet concentrations and flowrates were equal for the reference and maximum current conditions which provided the limits $1/2 < \bar{c}_s/\bar{c}_{sr} < 1$.

The maximum current densities were correlated by substituting experimental values for the dimensional parameters that appear in the groups listed in Equations 9–12. In particular, the normalized reactant concentration, K_c, characterizing the magnitude of the cathode overpotential was defined as

$$K_c = 2\left(\frac{c_{1r}}{c_{3L}}\right)\left(\frac{\bar{c}_s}{\bar{c}_{sr}}\right) \tag{28}$$

Here, the quantity c_{3L} is the cation concentration of the electrolyte at the anode. For example, a potassium pyrosulfate electrolyte used for SO_2 absorption

has a molecular weight of $M_w = 254$ and a density of $\rho = 2.28\,\mathrm{gm\,cm^{-3}}$. Assuming each mole of $K_2S_2O_7$ dissociates into two moles of cations, $c_{3L} = 2\rho/M_w = 0.019\,\mathrm{mol\,cm^{-3}}$.

The remaining concentration c_{1r} is the reference concentration of the current carrying ion located at the gas interface within the cathode. For the cases in Table 1 involving the adsorption of H_2S or CO_2, previous estimates were used of the rates on the cathode surface. The normalized reactant concentration K_c for the data covered the range of values $0.08 < K_c < 0.7$ representing small to moderate overpotentials where most of the data (with the exception of SO_2 absorption) is at roughly $K_c \simeq 0.5$.

As indicated in Table 1, the estimated ion diffusivities, electrolyte concentrations and cathode specific surface area were approximately constant for the dimensionless group K_c and $K_aK_h^2$. The lateral spread of the data in Fig. 4 was due largely to variations in the exchange current i_r (factor of 30). Most of the data (80%) lie within the envelope defined by lines of constant overpotential $0.1 < K_c < 1.0$ predicated by Equation 22. These data appear to follow the trend of the theory in spite of uncertainties in the estimation of ion diffusivities, electrolyte concentrations, exact chemical pathway for the production of the current carrying ion and the possibility of pore flooding and the subsequent reduction in cathode specific surface area.

Thirty five per cent of the selected data (H_2S absorption) lie significantly below the expected ideal current limit. Flooding of the electrode may be the problem for these data leading to increased polarization over time, reduced cathode specific surface area and reduced cell efficiency or ion transport. Other potential problems are the leakage of gaseous hydrogen to the anode through cracks in the membrane ceramic or support structure. These problems have been discussed in some detail [6, 10]. Therefore, selected data representing the maximum current for each of the three gases have been replotted in Fig. 5 on nondimensional coordinates of sulfide and carbonate content at $T = 640\,^\circ\mathrm{C}$ for the eutectic Li_2CO_3–K_2CO_3 [6]. Finally, the solubility limit of sulfate was used to estimate c_{1r} from McHenry and Winnick [10].

4. Discussion

It is important to note the significance of Equation 23 that predicts the maximum current density in the diffusion limit ($K_aK_h^2 \gg 1$). The transport of the current carrying ion across the membrane is the result of the combined effects of migration in the electric field plus molecular diffusion where the contribution of the former is proportional to the local ion concentration c_1. Moreover, at maximum current conditions c_1 in the cathode increases relative to the reference or open circuit value c_{1r}. Equation 23 illustrates that the same maximum current would result by assuming simple diffusion (no migration) across the membrane with the reference concentration c_{1r} in the cathode. This concept greatly simplifies both the calculation and interpretation of maximum current data. Figure 3 illustrates this concept by comparing a linear concentration profile across the membrane with the computed profile. These profiles predict the same current density to an accuracy of $O(K_c^2)$. The maximum current data are illustrated in Fig. 4 representing the normalized current limit against the ratio of ion diffusion : reaction time $K_aK_h^2$. The experimental data cover the range $0.06 < K_aK_h^2 < 1.5$ indicating that the current density limitations of the cell were affected by electrochemical reaction maximum current against reactant concentration. The solid line in Fig. 5 is Equation 20 valid for $K_aK_h^2 \gg 1$.

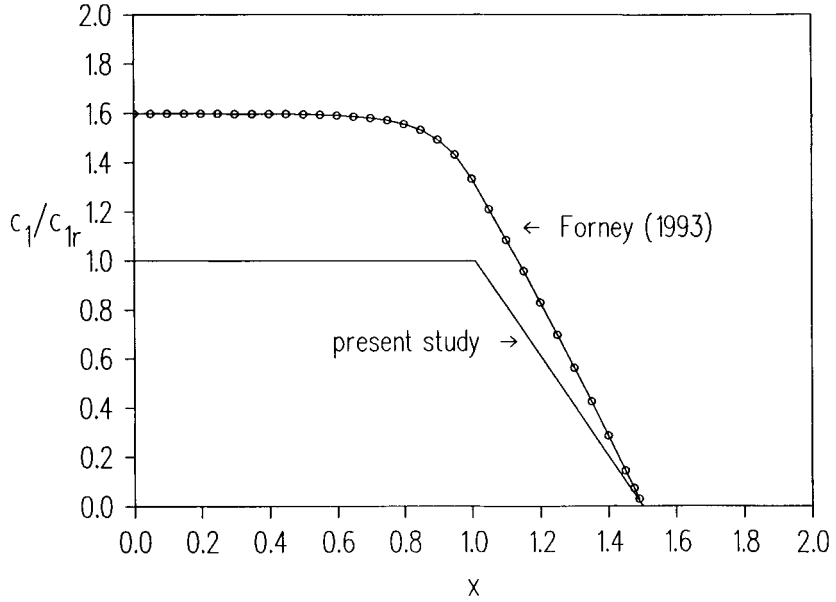

Fig. 3. Comparison of concentration profiles. The solid line provides approximately the same current as does the analytical solution (open circles). $K_h = 0.5$; $K_c = 0.4$; $K_a = 25$.

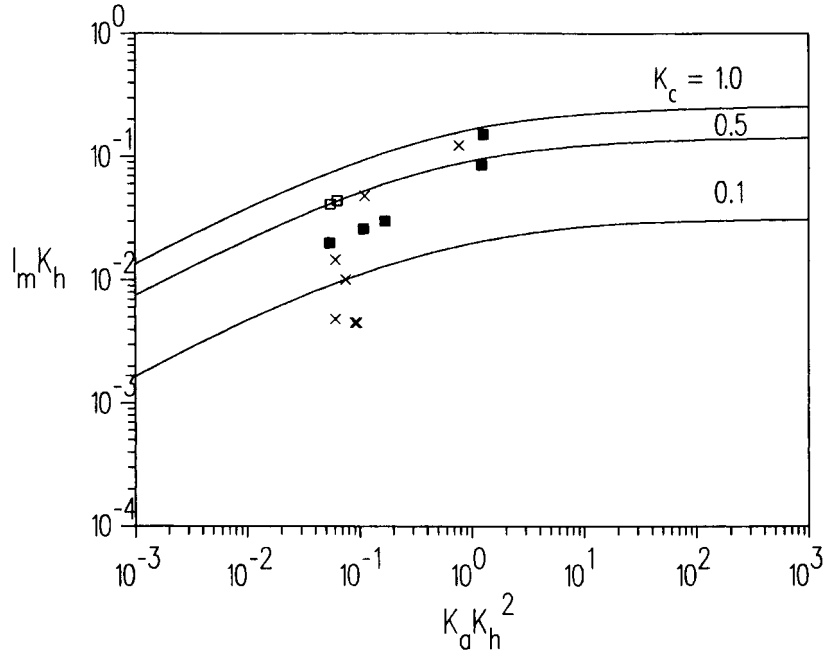

Fig. 4. Normalized current limit against the ratio ion diffusion : reaction time. Contours are lines of constant overpotential. See Table 1 for experimental data. Key: (×) H_2S; (■) CO_2; (□) SO_2.

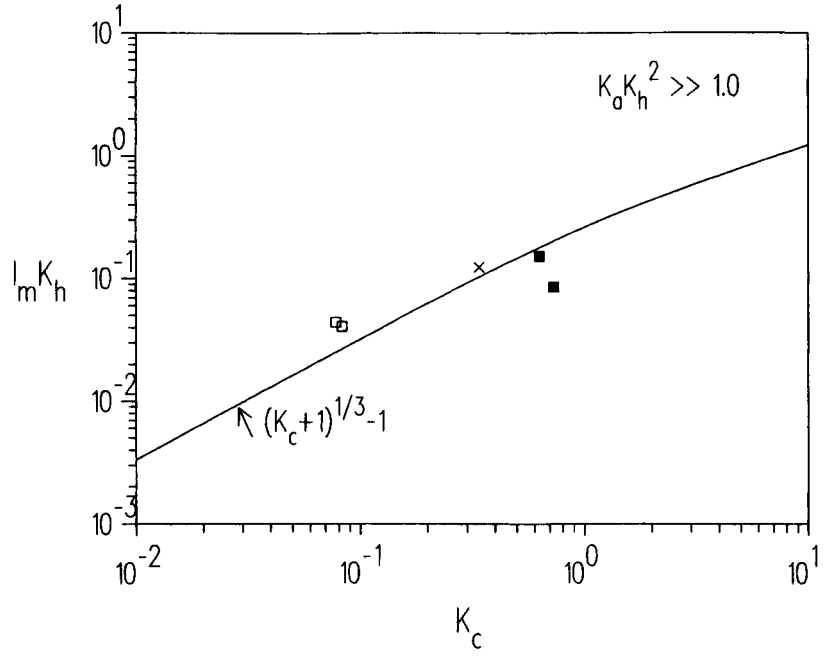

Fig. 5. Normalized maximum current against reference concentration of current carrying ion (overpotential). See Table 1 for experimental data. Key: (×) H_2S; (■) CO_2; (□) SO_2.

Substituting values for the dimensional parameters that appear in Equation 23 where $h_s = 0.2\,\text{cm}$, $c_{1r} = 0.008\,\text{mol cm}^{-3}$ ($M = 8$), $D_l^S = 1 \times 10^{-5}\,\text{cm}^2\,\text{s}^{-1}$ and assuming $1/2 < \bar{c}_s/\bar{c}_{sr} < 1$ for equal flowrates and reactant gas concentrations between reference and cell operating conditions, gives

$$i_m = \frac{2\left(8 \times 10^{-3}\,\text{mol cm}^{-3}\right)\left(9.6 \times 10^4\,\text{C mol}^{-1}\right)}{(0.2\,\text{cm})} \times \frac{\left(1 \times 10^{-5}\,\text{cm}^2\,\text{s}^{-1}\right)(0.5-1)}{(0.2\,\text{cm})}$$

or the maximum current density covers the range

$$i_m = 38 - 76\,\text{mA cm}^{-2}$$

The lower limit for the current density occurs when the gas phase reactant concentration $c_f/c_0 \to 0$ and $i_r/i_m \to 0$. It should be noted that the expected range of molarity for the salts used in the present study would cover $M = 9$ ($K_2S_2O_7$) to $M = 28$ (Li_2CO_3). It is unlikely that the concentration of the current carrying ion c_{1r} appearing in Equation 28 could exceed these limits for the dissociated molten salt.

5. Conclusions

A second order expansion has been used to correlate maximum current density data. The expression is valid for both small to large cathode electrode specific surface areas. The data correlated demonstrate that practical current density limitations of the cell are affected by electrochemical reaction rates on the cathode surface. For the case of large cathode specific area diffusion limit $K_a K_h^2 \gg 1$ and low to moderate overpotentials $K_c \leq 1$, the limiting or maximum current density is predicted for a gas diffusion electrode–membrane cell. The maximum current density in the latter case reduces to simple molecular diffusion (no migration) across the membrane with a uniform ion reference concentration c_{1r} (open circuit) in the cathode as the driving force. The simple model correlates the maximum current data for the absorbed gases $H_2S(S^{2-})$, $CO_2(CO_3^{2-})$ and $SO_2(SO_4^{2-})$.

The maximum current limit may be increased significantly by (i) increasing the concentration c_{1r} in the present system by either doping the electrolyte with an alkali metal salt containing the same anion or choosing electrolyte eutectic compositions with large solubility limits for the diffusing ion; (ii) increasing the ion diffusivity D_1^s by changing the electrolyte composition or temperature; (iii) designing thinner membranes that will retain the electrolyte and (iv) prevent electrode pore flooding by capillary action which appears to significantly reduce the cathode specific surface area.

References

[1] D. M. Bernardi and M. W. Verbrugge, *AIChEJ* **37** (1991) 1151.

[2] S. J. Ridge, R. E. White, Y. Tsau, R. N. Beaver and G. A. Eisman, *J. Electrochem. Soc.* **136** (1989) 1902.

[3] G. Wilemski, T. Wolf, D. Bloomfield, M. L. Finson, E. R. Pugh and K. L. Wray, 'Performance Model for Molten Carbonate Fuel Cells', Final Report, DDE DE-AC-03-79 ET11322; Physical Sciences, Inc.: Andover, MA (1979).

[4] S. H. Langer and R. G. Haldeman, *J. Phys. Chem.* **68** (1964) 962.

[5] L. Walke, K. Atkinson, D. Clark, D. Scardaville and J. Winnick, *Gas Sep. Purif.* **2** (1988) 72.

[6] S. Alexander and J. Winnick, *Sep. Sci. Technol.* **26** (1990) 2057.

[7] D. Weaver and J. Winnick, *J. Electrochem Soc.* **138** (1991) 1626.

[8] Z. Mao, P. Adanuvor and R. E. White, *ibid.* **137** (1990) 2116.

[9] L. J. Forney, *I & EC Research* **36** (1993) 1204.

[10] D. J. McHenry and J. Winnick, *AIChEJ* **40** (1994) 143.

[11] V. G. Levich, 'Physicochemical Hydrodynamics, Prentice Hall, Englewood Cliffs, NJ (1962), pp 293–6.

[12] R. F. Probstein, 'Physicochemical Hydrodynamics: An Introduction', Butterworths: Boston, MA (1989), pp 161–70.

[13] S. R. Alexander, 'Electrochemical Removal of H_2S from Fuel Gas Streams', PhD thesis, Georgia Institute of Technology (1993).

[14] D. J. McHenry, 'Development of an Electrochemical Membrane Process for Removal of SO_x/NO_x from Flue Gas', PhD thesis, Georgia Institute of Technology (1992).

[15] D. Weaver, Electrochemical Membrane H_2S Separator, PhD thesis, Georgia Institute of Technology (1988).

[16] G. J. Janz and N. P. Bansal, *J. Phys. Chem. Ref. Data* **11** (1982) 624.

[17] C. J. Geankoplis, 'Transport Processes and Unit Operations', 2nd edn, Allyn and Bacon, Newton, MA (1983), p. 391.